

Electronic Supplementary Information for
Macrophage-Mediated Delivery of Light Activated Nitric Oxide Prodrugs
with Spatial, Temporal and Concentration Control

Michael A. Evans,^{†,a,b,c} Po-Ju Huang,^{†,a} Yuji Iwamoto,^d Kelly N. Ibsen,^b Emory M. Chan,^e
Yutaka Hitomi,^d Peter C. Ford^{a,*} and Samir Mitragotri^{b,c,*}

^aDepartment of Chemistry and Biochemistry, University of California, Santa Barbara, Santa Barbara, CA, 93106 USA

^bDepartment of Chemical Engineering and Center for Bioengineering, University of California, Santa Barbara, Santa Barbara, CA, 93106 USA.

^cJohn A. Paulson School of Engineering and Applied Sciences, Harvard University, 29 Oxford St., Cambridge, MA 02138, USA

^dDepartment of Chemistry and Biochemistry, Doshisha University, 1-3 Tatara Miyakodani, Kyotanabe, Kyoto 610-0394, JAPAN

^e The Molecular Foundry, Lawrence Berkeley National Laboratory, Berkeley, CA USA

Table of Contents:

Figure S1. Quantum yield measurement for 794 nm photolysis of [Mn(dpaq^{NO₂})(NO)]BPh₄ (**I**) in acetonitrile.

Figure S2. SEM image and size distribution of PLGA microparticles loaded with [Mn(dpaq^{NO₂})(NO)]BPh₄ (**I**) and Nd-UCNPs.

Figure S3. Size distribution of micro-carriers PLGA-1 and PLGA-2 and NO release upon the 794 nm laser photolysis.

Figure S4. Comparison images of uptake of bare PLGA particles vs IgG labeled particles by immortalized J774.A1 macrophages.

Figure S5. DAF detection of intracellular NO release from particles

Figure S6. An illustration of macrophage chemotaxis in a transendothelial assay.

Figure S7. Representative images of tumor spheroids.

Figure S8. Comparisons of NIH-3T3/4T1 co-cultured spheroid sizes after 10 days of growth.

Figure S9. Flow cytometry analysis of macrophage infiltration into tumor spheroids.

Figure S10. Flow cytometry analysis of HIF-1 α content inside spheroids.

Figures

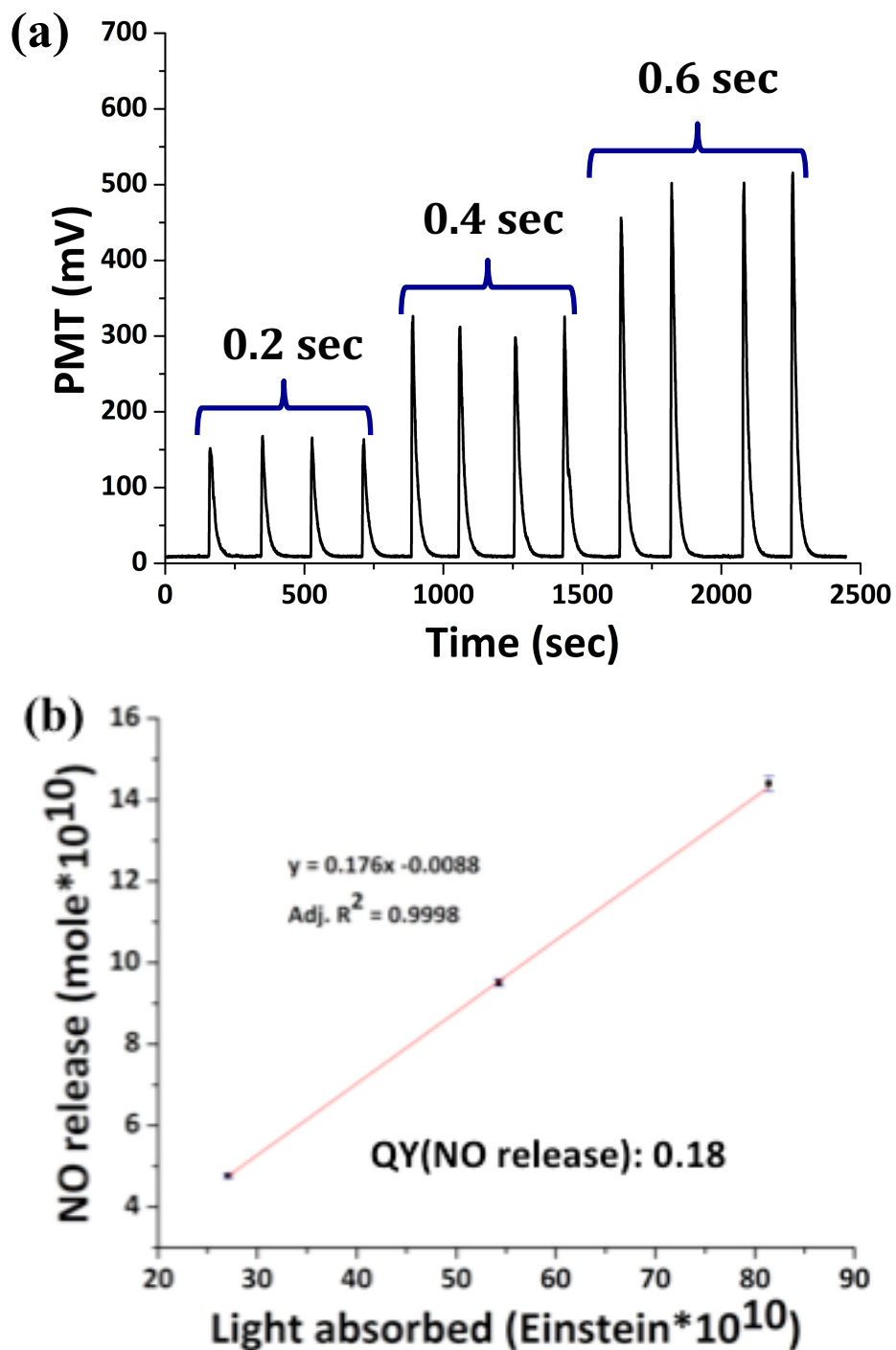


Figure S1. (a) NOA signals from the 794 diode laser photolysis of $[Mn(dpaq^{NO_2})(NO)]BPh_4$ in acetonitrile at 1.9 W/cm^2 intensity with different irradiation times (0.2, 0.4 and 0.6 sec). (b) Plot of NO detected vs light absorbed.

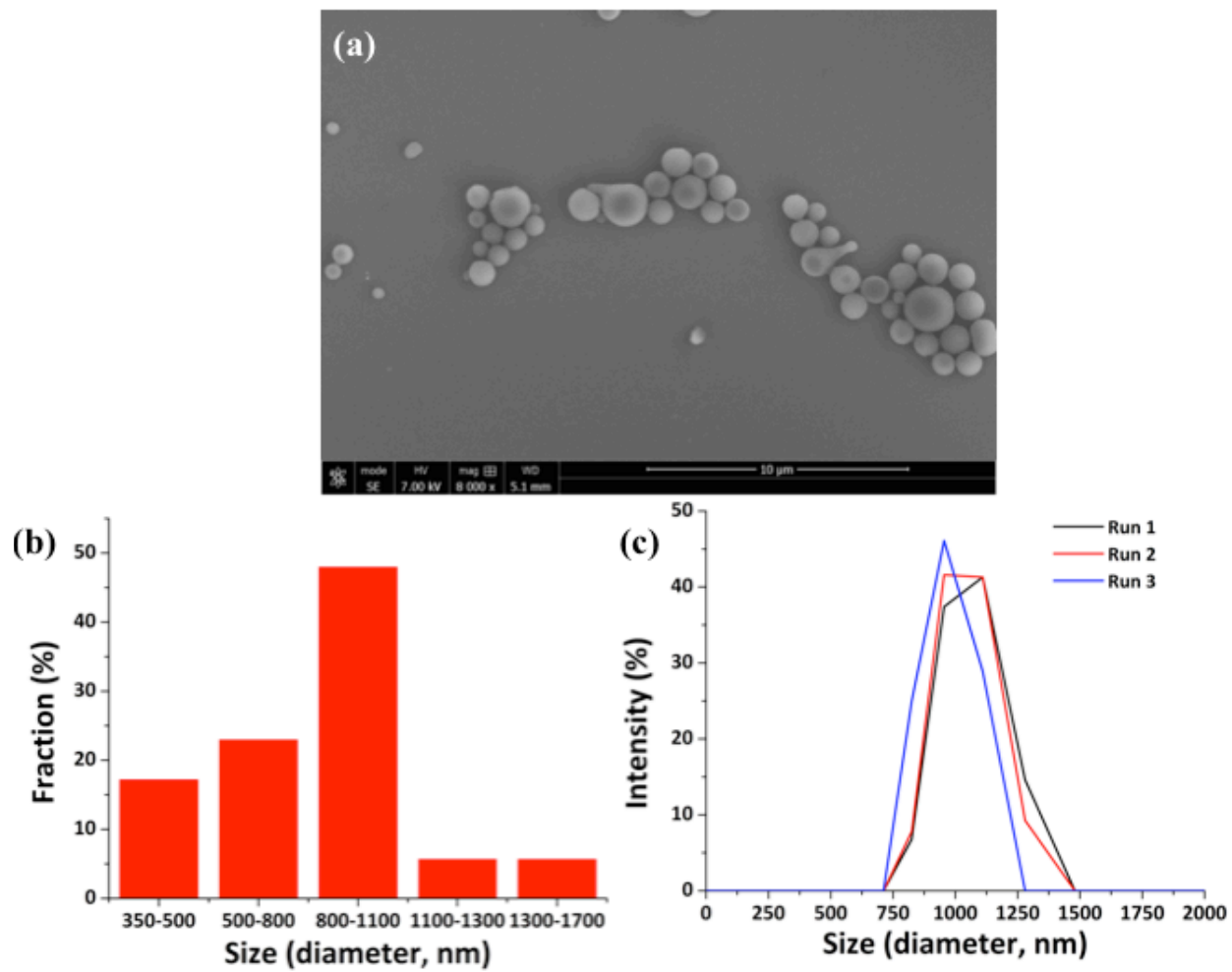


Figure S2. (a) The SEM image of PLGA microparticles loaded with $[\text{Mn}(\text{dpaq}^{\text{NO}_2})(\text{NO})]\text{BPh}_4$ (**I**) and Nd-UCNPs (scale bar = 10 μm). (b) and (c) Size distribution of the microparticles determined using imageJ and dynamic light scattering, respectively.

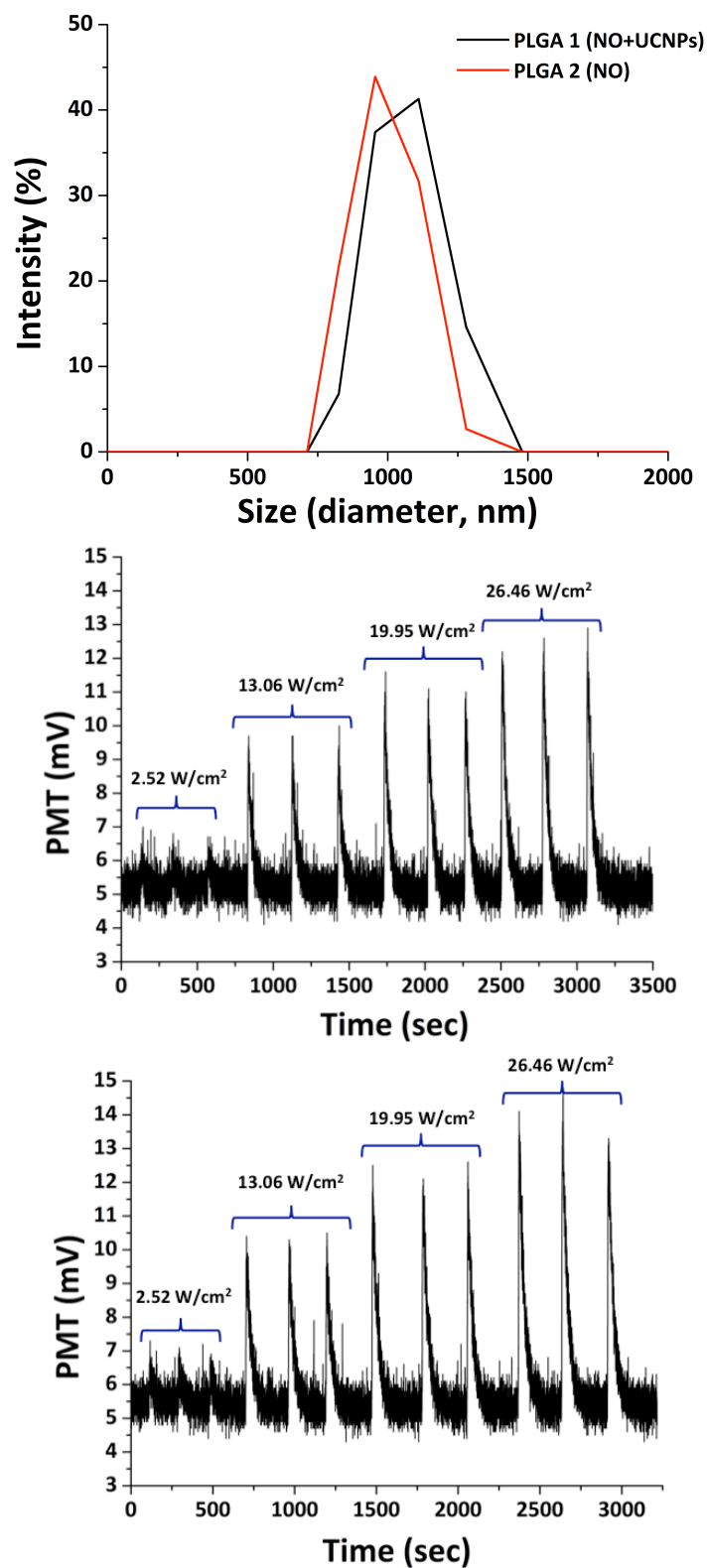


Figure S3. *Top:* Size distribution of the micro-carriers PLGA-1 and PLGA-2 as determined using dynamic light scattering. *Middle and Bottom:* NOA signals from the 794 diode laser photolysis of suspensions of PLGA-1 and PLGA-2, respectively, at different intensities in W/cm^2 .

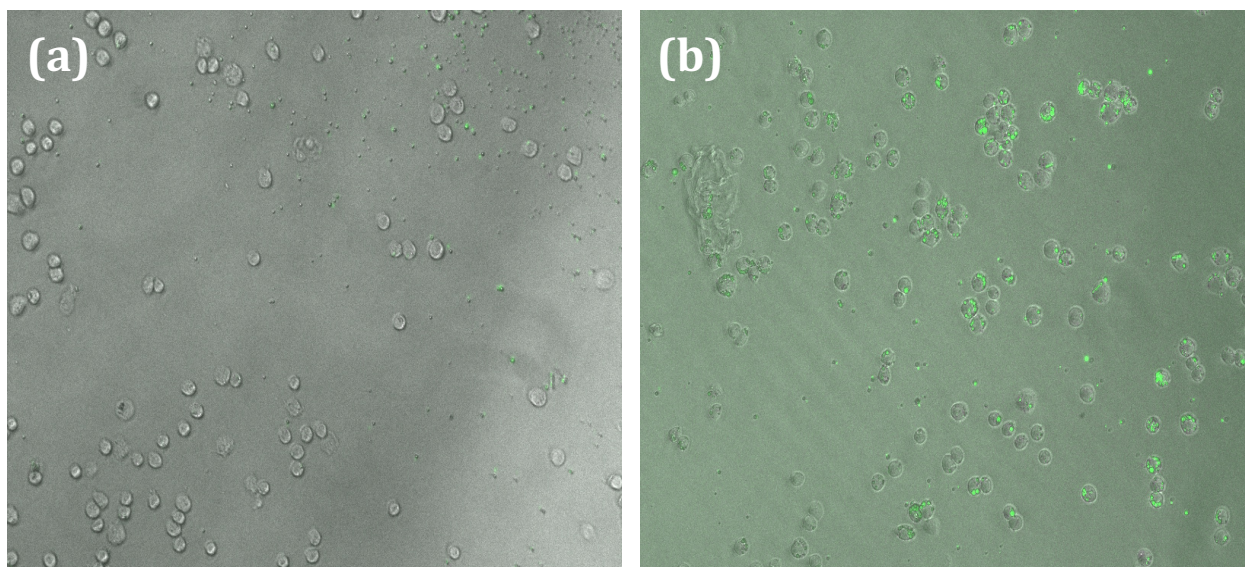


Figure S4. Comparison images of uptake of bare PLGA particles (a) and of IgG labeled particles (b) by immortalized J774.A1 macrophages at 150 $\mu\text{g}/\text{mL}$ particle concentration. Particles contained encapsulated coumarin 6 for visualization.

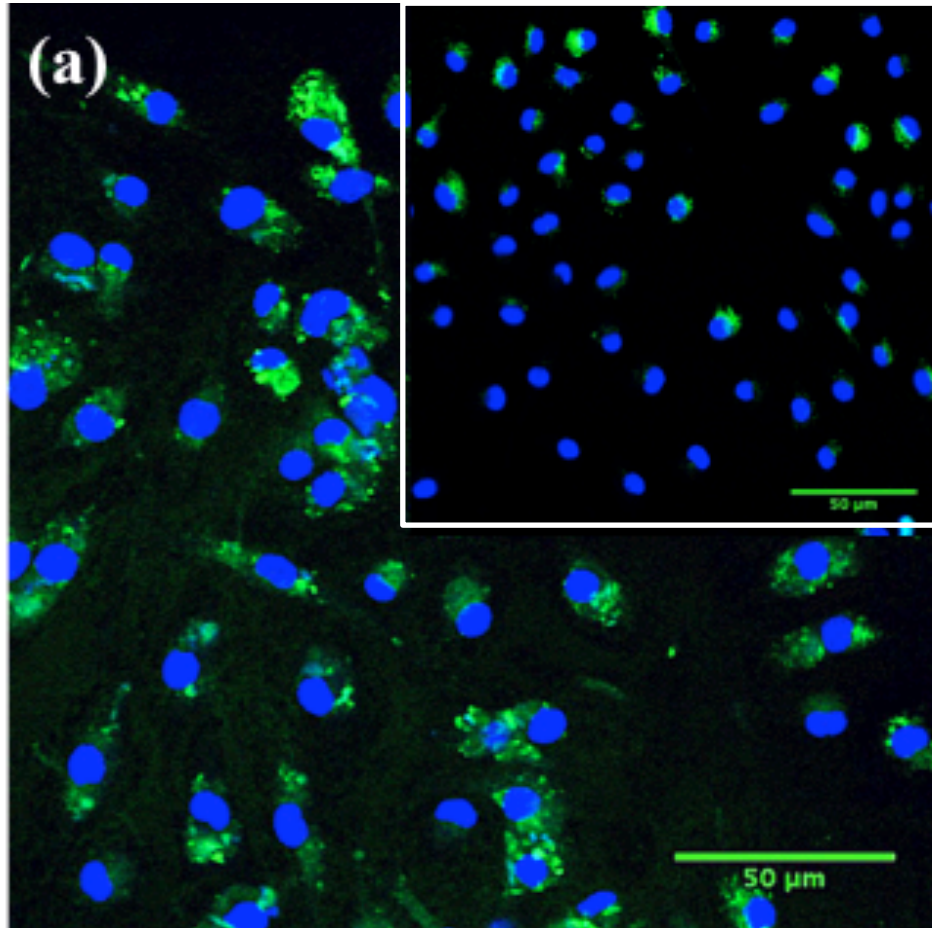


Figure S5. BMMp⁺ irradiated with a 794 nm diode laser for 90 s. The inset figure is the control experiment with BMMs only. NO was detected using 4-amino-5-methylamino-2',7'-difluorofluorescein diacetate (DAF-FM-2DA) fluorescent reporter (green color). (both samples were incubated with L-N^G-nitroarginine methyl ester (L-NAME) to inhibit endogenous NO generation.) Blue color is 4',6-diamidino-2-phenylindole (DAPI) stain.

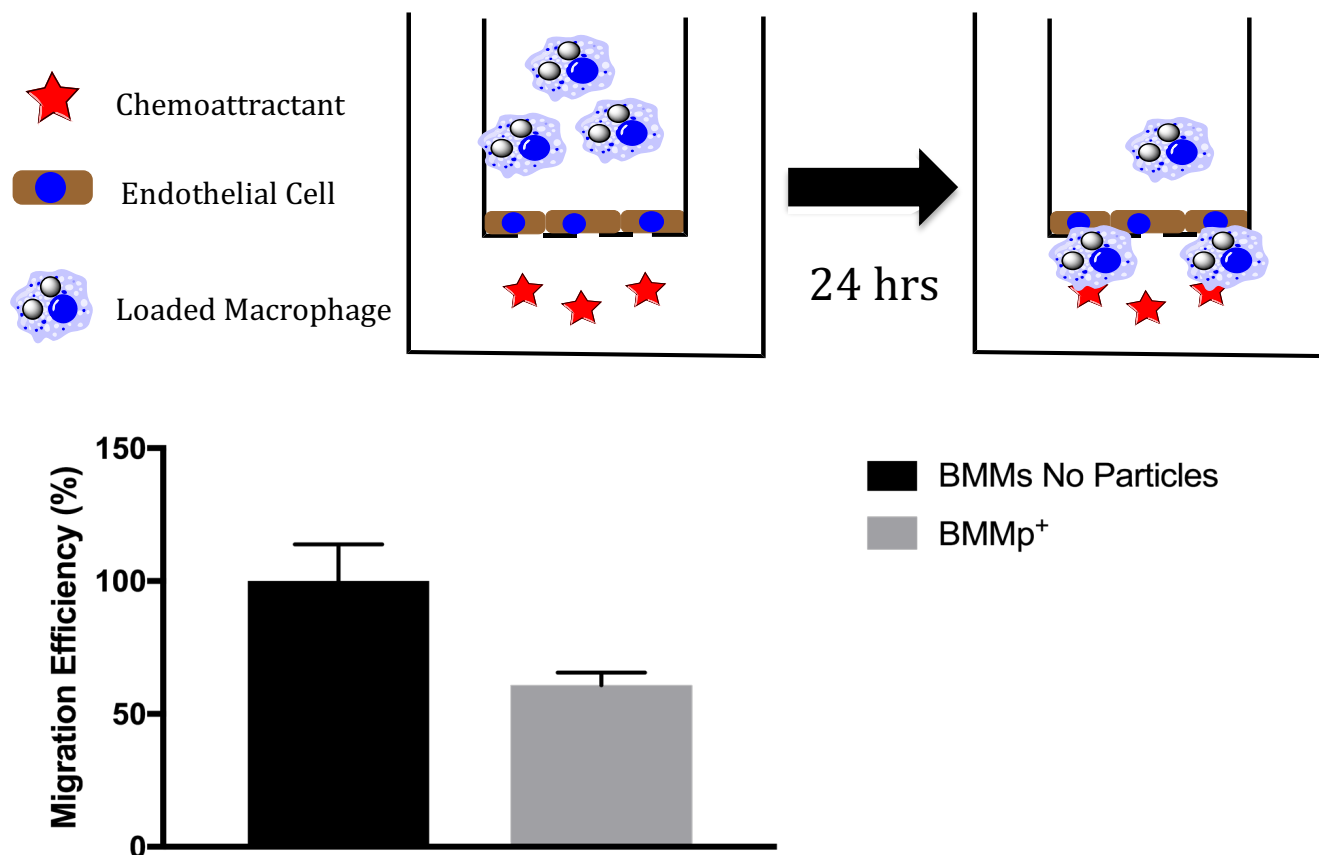


Figure S6. *Top:* An illustration of macrophage chemotaxis in a transendothelial assay. Macrophages are placed on top of the endothelial layer and MCP-1 on the other as a chemotaxic agent. Macrophages are attracted to the chemoattractant and traverse the endothelial monolayer. These cells are quantified by adding NucBlue[®] to stain the nuclei of cells that have crossed so they can be analyzed by counting cell nuclei with a fluorescent microscope. *Bottom:* Graph comparing the migration efficiency of macrophages with and without particles.

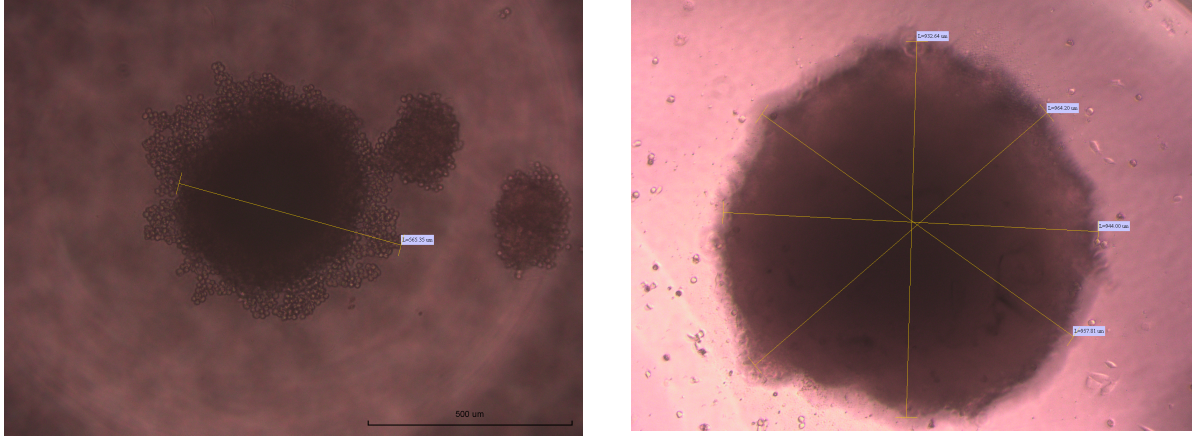


Figure S7. Representative images of tumor spheroids produced with 4T1 cells alone (left) or a 5:1 3T3:4T1 coculture method (right) after infiltration with particle loaded macrophages. Due to the density of the spheroids, particles cannot be seen in these images.

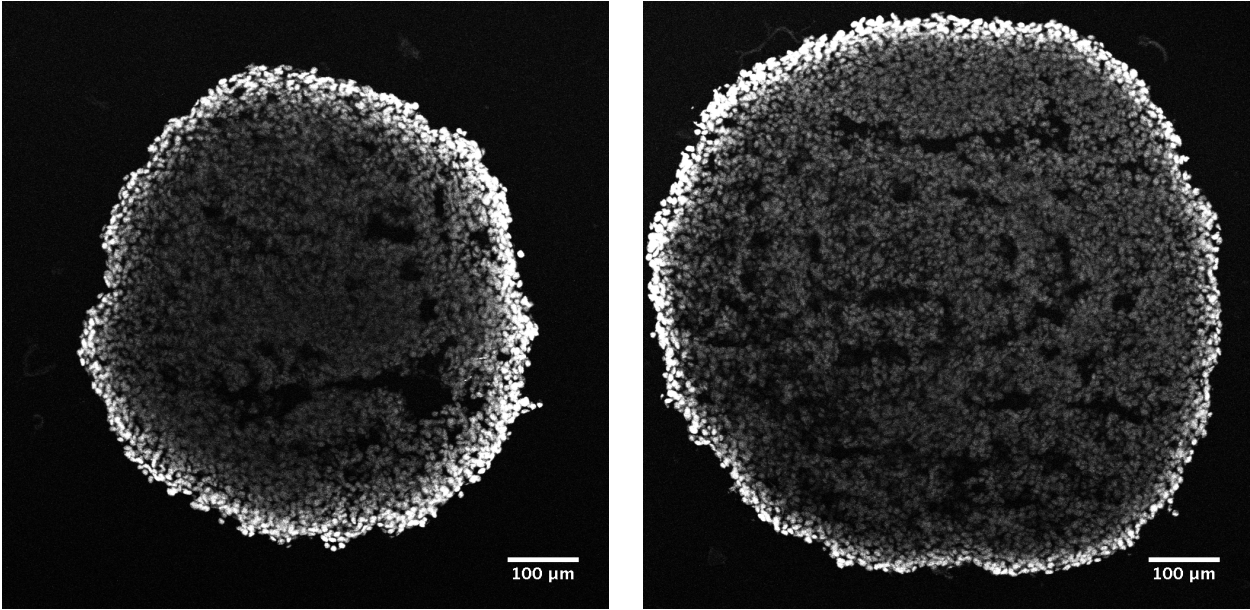


Figure S8. Comparisons of NIH-3T3/4T1 coculture spheroid size after 10 days of growth with (right) and without (left) macrophages introduced on day 7. Images represent center slices of tumor spheroids stained with DAPI acquired with a confocal microscope.

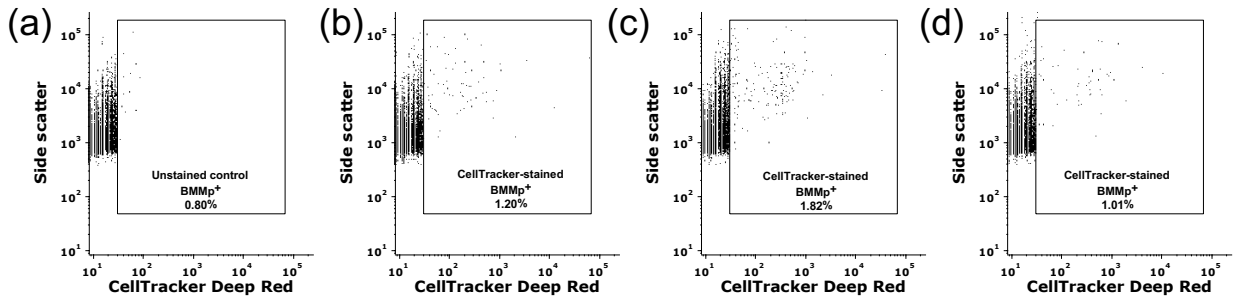


Figure S9. Flow Cytometry analysis of macrophage infiltration into tumor spheroids (b-d). Macrophages were labeled with CelltrackerTM deep red to allow for their identification. Results were subtracted from the proportion of gated cells in the control (a).

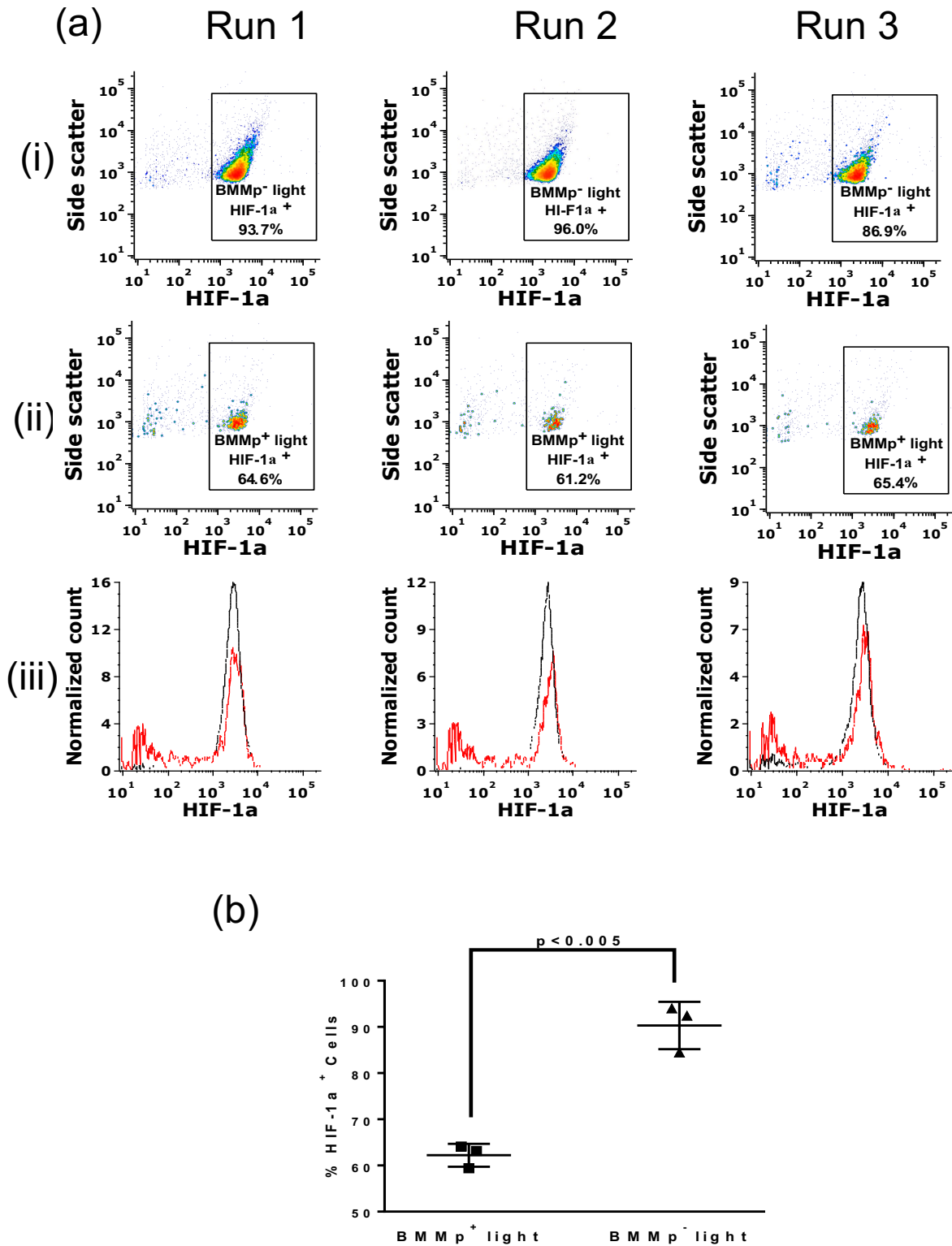


Figure S10. (a) Flow cytometry analysis HIF-1 α content inside spheroids containing (i) BMMp⁻ and (ii) BMMp⁺ after 7 hours of exposure to a 735 nm LED at 0.58 mW/cm². (iii) Comparisons of i (black) and ii (red) for each run. (b) Statistical analysis of HIF-1 α levels in spheroids from both groups.